Influence of randomness in topology, geometry and material properties on the mechanical response of elastic central-force networks

Reference:

Mühlich Uwe, Ballani Felix, Stoyan Dietrich.- Influence of randomness in topology, geometry and material properties on the mechanical response of elastic central-force networks

Probabilistic engineering mechanics - ISSN 0266-8920 - 40(2015), p. 36-41

DOI: http://dx.doi.org/doi:10.1016/j.probengmech.2015.02.005

Influence of randomness in topology, geometry and material properties on the mechanical response of elastic central-force networks[1]

Uwe Mühlich*
Institute of Mechanics and Fluid Dynamics, TU Bergakademie Freiberg.

Felix Ballani†
Institute of Stochastics, TU Bergakademie Freiberg.

Dietrich Stoyan‡
Institute of Stochastics, TU Bergakademie Freiberg.
(Dated: January 18, 2015)

We show that topological features have strong influence on the mechanical response of random elastic networks. In the simple case of a planar central force network under uni-axial compression, we vary first randomly topological characteristics under the condition that the numbers of nodes and edges in the network are fixed. Subsequently, we vary simultaneously topology and geometry and topology and local stiffness, respectively. It turns out that the characteristics related to topology determine the major trend in the mechanical behavior while randomness in geometry and local stiffness play a minor role.

I. INTRODUCTION

Random networks play an important role in modern materials modeling. Such networks consist of vertices, also called nodes, randomly distributed in space, which are connected by edges also known as bonds, see [1, 2]. A famous example is the network of edges of a Voronoi tessellation. Often the edges are equipped with physical properties such as mechanical stiffness or permeability. Such network models have proven to be useful for investigating effective properties of porous media and foams as documented by a large amount of literature, see for instance [3–7], just to mention a few.

Typically, the original structures are not networks. The transition to networks is usually done since for networks physical computations are simpler than with other approaches, for instance volumetric models. There are various methods for the construction of networks [8].

Having selected a particular network model, the materials structure is captured to a large extent by the geometrical and topological properties of the network's node-edge system. In addition, further geometrical properties are assigned to the edges like curvature and distribution of cross-section area as well as physical properties like stiffness, yield stress, etc. [9].

In the recent literature, the choice of a specific network model is usually based on a limited number of real material samples as in [10–14]. Only little variation of geometry and/or topology is usually possible and dictated by the variability of the materials studied. Therefore, it is difficult to generalize results and to find out which geometrical-topological network properties dominate the physical response, for instance permeability or mechanical stiffness. Especially the effect of network topology on the physical response seems far from being understood although the importance of topological features was reported implicitly already in [15]. A possible reason may lie in the fact that topological features can hardly be controlled independently in more complex random networks.

The present paper is an attempt to attack this problem. In a case study, attention is focused on the response of planar elastic central-force lattice networks under mechanical load. Such networks have been investigated already in the spirit of solid state physics for example in [16–21] about twenty years ago. Investigations focused on strength of materials and structural mechanics, respectively, are reported for instance in [22–24]. However, the influence of topology on the physical response, if any, plays only a minor rule even in these papers.

We fix the number of nodes and edges, in order to circumvent trivial statements of the type that networks become stronger with increasing number of edges. This implies that a major topological characteristic, the network's Euler number, is fixed. However, characteristics which describe local topological fluctuations are varied in our study.

II. PROBLEM DEFINITION

We consider networks constructed starting from a regular lattice of nodes. The nodes are connected by horizontal and vertical edges of length l yielding an arrangement of square cells. Every cell is equipped with exactly one diagonal edge the direction of which is random. We will speak about "lattice networks".

Our networks are interpreted as periodic arrangements

* muehlich@imfd.tu-freiberg.de
† ballani@math.tu-freiberg.de
‡ stoyan@math.tu-freiberg.de
[1] Author's version of the article published in Prob. Eng. Mech. 40 (2015) 3641, doi:10.1016/j.probengmech.2015.02.005

of a basic pattern, which consists of $M \times M$ cells as shown in Fig. 1. The latter is shifted by a vector $\underline{\boldsymbol{d}}$

$$\underline{\boldsymbol{d}} = p\lambda\,\underline{\boldsymbol{e}}_1 + q\lambda\,\underline{\boldsymbol{e}}_2 \tag{1}$$

with $\lambda = Ml$ and arbitrary integers p and q ($p, q \in \mathbb{Z}$) in order to obtain an area-filling tessellation.

The nodes are interpreted as pin joints and the edges as linear elastic rods, also called trusses. Cross section area A as well as Young's modulus Y are assumed to be constant within a rod.

We consider an overall strain state, defined via an effective strain tensor $\boldsymbol{E}$. As long as the physical response is periodic too, simulations can be performed by means of the $M \times M$ basic pattern. In order to enforce periodicity, the boundary conditions are prescribed as follows. The displacement vector at node (i, j) is split into a linear part and a fluctuation

$$\underline{\boldsymbol{u}}_{(i,j)} = \boldsymbol{E} \cdot \underline{\boldsymbol{X}}_{(i,j)} + \underline{\tilde{\boldsymbol{u}}}_{(i,j)} \tag{2}$$

where $\underline{\boldsymbol{X}}_{(i,j)}$ is the position vector of node (i, j) in the undeformed configuration given by

$$\underline{\boldsymbol{X}}_{(i,j)} = [j-1]l\,\underline{\boldsymbol{e}}_1 + [i-1]l\,\underline{\boldsymbol{e}}_2 \quad i, j = 1, 2, ... \tag{3}$$

with the orthonormal base vectors $\underline{\boldsymbol{e}}_i$ as indicated in Fig. 1. The position vector of a node obtained from node (i, j) by shift $\underline{\boldsymbol{d}}$ can be expressed as

$$X_{(i+pM,j+qM)} = X_{(i,j)} + q\lambda\underline{\boldsymbol{e}}_1 + p\lambda\underline{\boldsymbol{e}}_2\,. \tag{4}$$

Hence, the displacement vector at this node is

$$\begin{aligned}\underline{\boldsymbol{u}}_{(i+pM,j+qM)} = \boldsymbol{E} \cdot [\underline{\boldsymbol{X}}_{(i,j)} + q\,\lambda\,\underline{\boldsymbol{e}}_1 + p\,\lambda\,\underline{\boldsymbol{e}}_2] \\ + \underline{\tilde{\boldsymbol{u}}}_{(i+pM,j+qM)}\,.\end{aligned} \tag{5}$$

Periodicity of the mechanical response in terms of kinematics is ensured by enforcing equal fluctuations for those nodes which are related by shift $\underline{\boldsymbol{d}}$ (see (1))

$$\underline{\tilde{\boldsymbol{u}}}_{(i,j)} = \underline{\tilde{\boldsymbol{u}}}_{(i+pM,j+qM)}\,, \tag{6}$$

from which

$$\underline{\boldsymbol{u}}_{(i+pM,j+qM)} = \underline{\boldsymbol{u}}_{(i,j)} + \boldsymbol{E} \cdot \lambda[q\underline{\boldsymbol{e}}_1 + p\underline{\boldsymbol{e}}_2] \tag{7}$$

follows. In order to avoid rigid-body motion, the displacement vector at the lower left node $\underline{\boldsymbol{u}}_{(1,1)} = \underline{\boldsymbol{0}}$ is prescribed. The displacement vectors at the three remaining corners are prescribed according to (7). At all other boundary nodes, (7) is enforced in terms of a constraint. The displacements at these nodes form part of the solution. Full periodicity of the mechanical response implies also constraints with respect to the reaction forces $\underline{\boldsymbol{R}}_{(m,n)}$ dual to the imposed kinematic constraints. Therefore,

$$\underline{\boldsymbol{R}}_{(i+pM,j+qM)} = -\underline{\boldsymbol{R}}_{(i,j)} \tag{8}$$

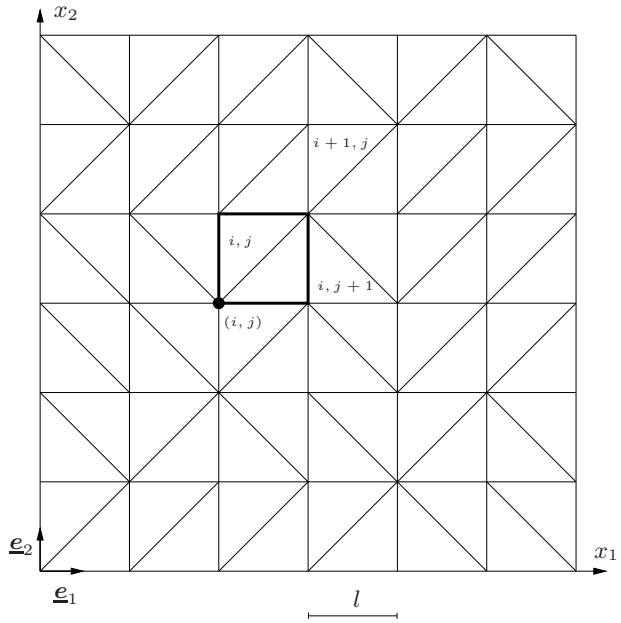

FIG. 1. Truss structure with random topology induced by randomness of diagonal directions together with the notation and the coordinate system used. Index pairs refer to cells and the corresponding diagonals, whereas index pairs within parentheses refer to nodes.

is enforced with respect to the reaction forces at all boundary nodes except at the corners. Regarding the latter, (8) is automatically fulfilled by the equilibrium solution.

In order to compute the response of the networks a finite-element scheme has been developed specifically for this purpose, following the standard procedure as given e.g. in [25]. It is worth noting that deviations from the exact solution are only due to floating point operations because the loading is exclusively applied at the nodes. Since uni-axial compression in x_2-direction is considered, all components of $\boldsymbol{E}$ vanish except E_{22}, for which $E_{22} = -0.05$ was set for all simulations, which corresponds to a vertical compression of 5%. We discuss the mechanical response in terms of the strain energy density of the lattice per M^2, denoted by W. This way networks can be classified according to their mechanical response by a single scalar measure regardless of different degrees of anisotropy. Furthermore, W remains a valid measure also in the case of multi-axial loading.

W is given by summing up the strain energies of the individual rods

$$W = \frac{1}{M^2}\sum_{e=1}^{N}\frac{1}{2}\frac{L_e}{l_e}\varepsilon_e^2 \tag{9}$$

where $N = M^2 + 2M(M+1)$ is the total number of rods in the structure and ε_e is the strain of rod e, computed from the displacements obtained by the finite-element approach mentioned above . L_e is the stiffness of the rod e given by the product of individual Young's modulus

and cross section area, $L_e = Y_e \cdot A_e$. Note that in a force-controlled test, a lower strain energy corresponds to a higher stiffness whereas for the strain-controlled setting used here, a lower W implies lower stiffness.

We consider three types of randomness: randomness in

(i) topology is introduced by randomness in directions of diagonal edges;

(ii) geometry is generated by moderate random shifts of the coordinates of the inner nodes around their lattice positions;

(iii) local stiffness is realized by choosing rod stiffness L_e randomly in the range $\bar{L} \pm 0.1\bar{L}$ using a uniform probability distribution for a fixed $\bar{L}$.

The three types of randomness can be generated separately or in combination. Note that even for our rather simple networks, topology cannot be varied completely independent from geometry. Since direction is a geometrical property, the change in topology is accompanied by some change in geometry. However, there is a significant difference between changes in direction and geometrical variation of node coordinates because the latter does not change topology at all.

Because rod stiffness is defined as Young's modulus multiplied by cross-section area, the variation in rod stiffness can be interpreted as a variation of material behavior or cross-section geometry or both. In all cases without randomness in stiffness, periodicity is ensured by using half of the stiffness for the rods along the boundary of the lattice. In cases with random rod stiffness, the same stiffness value was used for corresponding rods along opposite boundaries.

III. CHARACTERISTICS OF LATTICE NETWORKS

Every lattice network in our sense or "configuration" X_k ($k = 1...2^{M^2}$) is completely characterized by a discrete field $\{\xi_{i,j}\}$ with $i, j = 1, .., M$ and

$$\xi_{i,j} = \begin{cases} 0 \\ 1 \end{cases} \quad \text{if diagonal } i,j \quad \begin{matrix} / \\ \backslash \end{matrix} \ . \tag{10}$$

Therefore, a random lattice network can be characterized by random field characteristics. The first-order characteristic is the mean of $\{\xi_{i,j}\}$

$$\rho = < \xi_{i,j} > = \frac{1}{M^2} \sum_{i,j} \xi_{i,j} \, . \tag{11}$$

Geometrically, ρ is a directional characteristic, the ratio between the numbers of "/" and "\" diagonals. A simple second-order characteristic is

$$\mu = < \mu_{i,j} > \tag{12}$$

with

$$\mu_{i,j} = \sum_{\substack{k,l \\ d=1}} (\xi_{i,j} - \xi_{k,l})^2 \tag{13}$$

where $d = |i-k| + |j-l|$, i.e. the summation goes over the nearest-neighbor cells. Hence, $\mu_{i,j}$ measures locally some spatial correlation. Its mean, μ, captures in some extent the irregularity of a configuration.

We expect that ρ and μ control mainly the mechanical response W.

IV. SAMPLING STRATEGY

Even for moderate values of M there exists an intractable amount of possible configurations. Therefore, we sample in the space of possible lattice networks with prescribed values of ρ and controlled values of μ. For this purpose, we use the $M \times M$ Ising model with fixed magnetization as defined in [26, 27]. The spin variables in this model are interpreted as the directions of diagonals. According to [28], we write the probability distribution of the model as

$$P(X = X_k) = \frac{1}{Z} \exp(-\beta \mu(X_k)) \tag{14}$$

with partition function Z. As above, X_k denotes a configuration, $\mu(X_k)$ is μ as in (12) for X_k and β is the control parameter of the model. By means of β, the degree of regularity/irregularity of the configurations can be controlled. In our case, "regularity" refers to regularity in terms of the directions of the diagonal rods.

Samples are generated by simulating according to (14) employing the Metropolis algorithm constraint by ρ as described in [27], including picking pairs of spins. While ρ can be controlled directly, μ is only controlled indirectly via the β in (14). Thus, we arrive at a two-parameter model, with the parameters β and ρ.

V. RESULTS AND DISCUSSION FOR LATTICE NETWORKS

A. Overall stiffness

Fig. 2 shows the influence of the network size given by M on the scatter in strain energy density W for the most unfavorable case, i.e $\rho = 0.5$ and $\beta = 0$. Every box plot in Fig. 2 corresponds to fifty realizations with random diagonal directions, regular node coordinates and constant local stiffness. The coefficient of variation is less than 0.05, hence acceptably small, for $M \geq 20$. Therefore, $M = 20$ is sufficient to generate representative networks and used in the sequel.

Since the mechanical response is symmetric with respect to $\rho = 0.5$,

$$\bar{\rho} = \min(\rho, 1 - \rho) \tag{15}$$

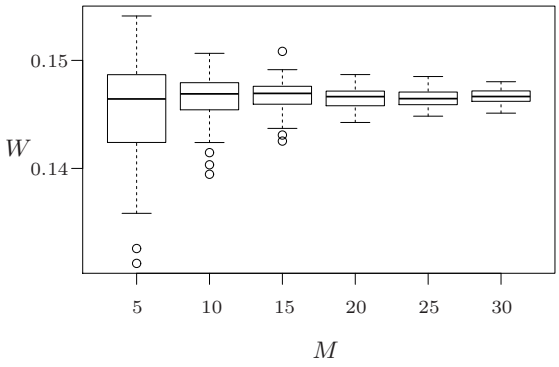

FIG. 2. Box plots showing the influence of the size of the networks M on the variability of the mechanical response W for $\rho = 0.5$ and $\beta = 0$. Every box plot corresponds to fifty realizations with random diagonal directions, regular node coordinates and constant local stiffness.

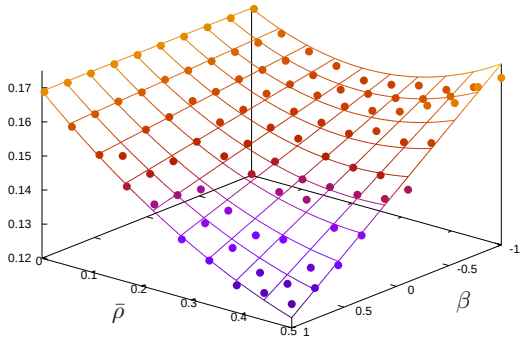

FIG. 3. Strain energy density W as function of the parameter β, which controls the degree of regularity/irregularity in terms of diagonal directions, and the directional ratio $\bar{\rho}$ (15). The grid represents the polynomial fit of the data points.

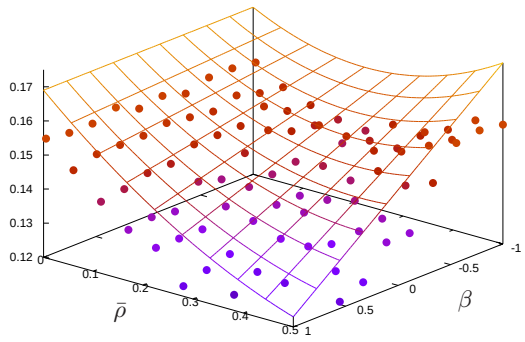

FIG. 4. Strain energy density W as function of the parameter β, which controls the degree of regularity/irregularity in terms of diagonal directions, and the directional ratio $\bar{\rho}$ (15). Here, also the coordinates of the nodes are varied at random. The grid from Fig. 3 serves as visual aid.

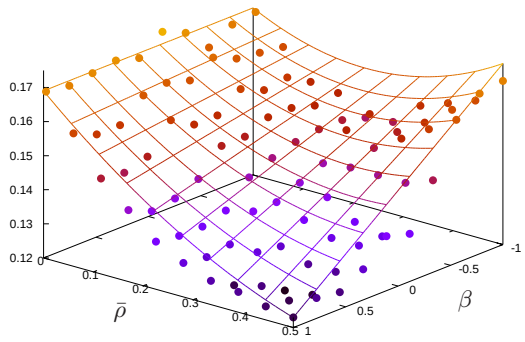

FIG. 5. Strain energy density W as function of the parameter β, which controls the degree of regularity/irregularity in terms of diagonal directions, and the directional ratio $\bar{\rho}$ (15). In addition, edge stiffnesses are varied. The grid from Fig. 3 serves as visual aid.

is used in the following. The results shown in Fig. 3, obtained by varying exclusively ρ and β show a strong correlation between the network's mechanical response and these two parameters. Every dot in Fig. 3 corresponds to the result for one particular configuration while the grid indicates a polynomial fit based on these data. For configurations with $\bar{\rho}$ close to zero, all or at least most of the diagonals have the same direction. Also the configurations with $\bar{\rho} = 0.5$ and $\beta = -1$ are perfectly regular but here, the direction of the diagonals alternates. Fig. 3 shows that an increase in topological irregularity causes a decrease in strain energy density, respectively a weaker structure.

In a next step, not only β and ρ are varied but in addition also the coordinates of the nodes which are uniformly scattered in squares of side-length $\frac{l}{2}$. The results are shown in Fig. 4, where the grid is the same as in Fig. 3 and serves as a visual aid to show that the parameters $\bar{\rho}$ and β determine the trend and that geometrical variation only causes a shift in the strain energy density and an increase in noise. Similar conclusions can be drawn from the results obtained by varying β and ρ together with the stiffness of the rods, see Fig. 5. Here again, the grid is same as in Fig. 3.

B. Failure onset

The results discussed so far indicate that regular configurations are stiffer than those with an irregularity induced by randomness of certain features. This observa-

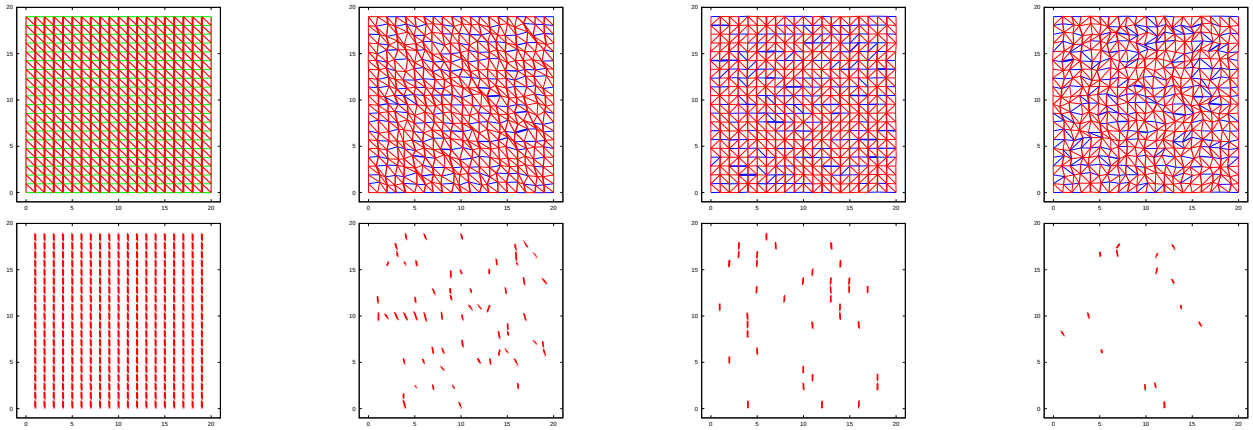

FIG. 6. Illustration of the effect of irregularity, respectively randomness, on the onset of failure. From left to right the deformed states are shown for a perfectly regular network, a network with the same topology but a random variation of the geometry, a network with irregular topology but regular geometry followed by a network with same topology but randomized geometry. In the second row, only the rods with 90 percent or more of the maximum stress are shown for the corresponding networks. A red color indicates compression stress whereas blue means tension. Finally, green is used for edges with zero stresses.

tion may give rise to the conclusion that randomness is a disadvantage as far as stiffness is concerned. However, the situation changes completely if failure is considered. At least for strain-controlled loading, randomness can be beneficial.

Complete failure of a configuration requires failure of a number of rods by which the structure becomes a kinematic mechanism. A rod fails if the stress, computed by the traction/compression force in the rod divided by the cross section area reaches a critical value. Although regular configurations will fail at higher overall strain, this failure will be sudden and catastrophically because the critical stress is reached in most of the rods for the same overall strain. Irregularity on the other hand may reduce the number of rods which experience the highest stresses. Furthermore, as shown in Fig. 6, the distances between the rods with high stresses are influenced by the irregularity. This illustrates that the linear elastic response provides already valuable information on the failure behavior. Therefore, it seems rather promising to exploit this information by generating point fields from the information about the rods with maximum stress in the network. This would allow for applying ideas provided by the theory of point processes.

VI. TRANSITION TO GENERAL NETWORKS

In this paper we consider a special class of planar networks that are constructed based on a lattice. The corresponding descriptors ρ and β are closely related to this construction. Since our final aim is to contribute to a general theory for planar networks, we show now that the lattice-based parameters ρ and β can be replaced by characteristics γ and σ_f that make sense for general networks. We show that these new characteristics yield similar statements for our lattice-based networks.

Since ρ characterizes directions, we recommend to replace it by an orientation measure. The following characteristic γ is inspired by directional statistics, [29], and is defined by

$$\tan\gamma = \frac{\sum_{e=1}^{N} l_e \sin\alpha_e}{\sum_{e=1}^{N} l_e \cos\alpha_e}\,, \tag{16}$$

where N is the total number of rods in the network, l_e the length of rod e and α_e the angle between the rod e and a given reference orientation, defined in such a way that the α_e are between $-\frac{\pi}{2}$ and $\frac{\pi}{2}$. We call it "mean relative direction". For all our lattice networks it holds

$$\tan\gamma = 1 - 2\rho\,, \tag{17}$$

if vertical and horizontal rods are dropped. In addition, the mean relative direction is zero for isotropic networks.

As a second characteristic, we propose the variance of the node degree. The latter counts the number of rods connected by a node [1]. Due to the construction of our networks, its mean is the same for all configurations. However, its variance, here denoted by σ_f^2, seems to be a suitable choice as it is variable [30].

In the following, the results obtained for the very same samples as used in Fig. 3 and Fig. 4 are rediscussed in terms of γ and σ_f^2. Before, some words about the relationship between β, $\bar\rho$ and σ_f^2. Fig 7 shows σ_f^2 as a function of β and $\bar\rho$. We see that both variables control σ_f^2 in a nonlinear way.

The strain energy for the samples which correspond to a variation of the diagonal directions, used previously in Fig. 3, is now interpreted by means of γ and σ_f^2. The result is shown in Fig. 8. It indicates that γ and σ_f^2 are as suitable as β and $\bar\rho$. Of course, the range of definition

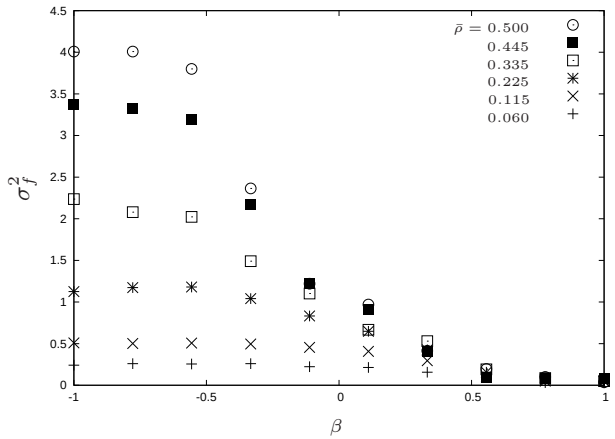

FIG. 7. Relation between σ_f^2 and β for various values of $\bar{\rho}$.

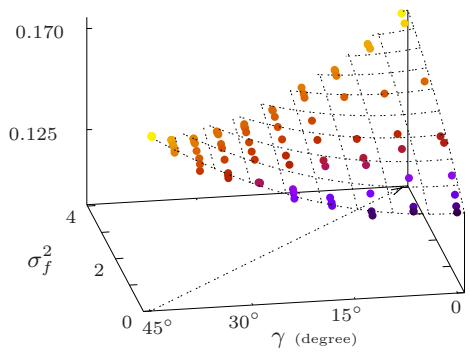

FIG. 8. Strain energy density W as function of the mean relative direction γ with respect to the reference orientation $\underline{\boldsymbol{e}}_2$ and the variance of the node degree σ_f^2. The sample is the same used for Fig. 3. The grid serves as visual aid.

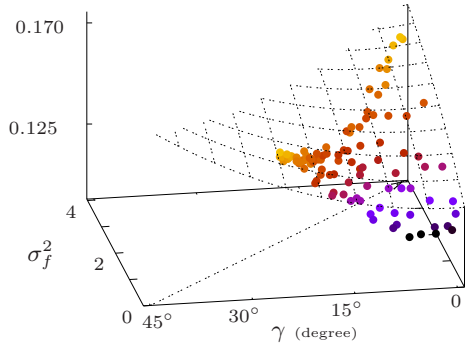

FIG. 9. Strain energy density W as function of the mean relative direction γ with respect to the reference orientation $\underline{\boldsymbol{e}}_2$ and the variance of the node degree σ_f^2. The sample is the same used for Fig. 4. The grid is the same as in Fig. 8 and serves as visual aid.

of γ and σ_f^2 is triangular, data points with $\gamma = 45°$ and $\sigma_f^2 = 0$ correspond to perfectly regular networks where all diagonals have an angle of 45°. Regular networks with alternating diagonals correspond to $\gamma = 0$ and $\sigma_f^2 = 4$.

Also the influence of random variations of the coordinates of the nodes is reproduced correctly if γ and σ_f^2 are used. This can be seen by comparing Fig. 8 and Fig. 9, where the latter contains the data of the networks for which topology and geometry are varied simultaneously at random. Hence, γ and σ_f^2 lead to the same conclusions as before, namely randomness in topology decreases the stiffness and simultaneous variation of topology and geometry causes a shift of the strain energy together with an increase in scatter whereas the general trend in W is maintained.

VII. DISCUSSION AND CONCLUSIONS

Our results show a strong correlation between the network's mechanical response W and the two model parameters ρ and β of the Ising model. If, in addition, geometrical randomness or randomness in local stiffness is taken into account, the response of the network shows the same trend with respect to ρ and β, although the results are quantitatively different and show significantly more noise. Since ρ and β control topology and direction, the results indicate that topology determines to a large extent the trend in stiffness of our networks. This suggests that topology should be one of the primary subjects of investigations regarding general networks.

Similar results were observed by reinterpreting the results in terms of mean relative direction γ and variance of the node degree σ_f^2. Probably the directional characteristic γ is useful in general for all planar networks, while it is clear that σ_f^2 is not always a suitable characteristic for topological variation. Indeed, in the case of a Voronoi tessellation the node degree is constant and the "dual" characteristic, variance of node number per cell σ_n^2, should be used. However, in the case of Delaunay tessellations, again σ_f^2 is suitable.

Here, only the results for uni-axial compression are presented. However, simulations were performed as well as for bi-axial compression and simple shear. We obtained similar results, leading to the very same conclusions.

We interpret our approach as a first step in the development of a strategy to find the topological-geometrical characteristics with major influence on the mechanical response of planar and spatial networks. Our investigation can be interpreted as one of second-order nature if we interpret the Euler number χ or the total length of all edges as first-order characteristics. The latter dominate in general the physical response, but this will be often nearly trivial. We are sure that the characteristics χ, σ_f^2 or σ_n^2, according to the particular class of networks, and γ will turn out as the characteristics of main interest.

Finally, as Fig. 6 and the discussion in section V B show, the linear elastic response of a network is closely

related to the failure behavior, at least to the onset of failure.

ACKNOWLEDGMENTS

This work was motivated by investigations related to the Collaborative Research Centre 799 funded by Deutsche Forschungsgemeinschaft and partially supported by the latter.

[1] M. Newman, SIAM Review **45**, 167 (2003)
[2] R. Albert and A.-L. Barabasi, Rev. Mod. Phys. **74** (2002)
[3] D. Weaire and M. Fortes, Adv. Phys. **43**, 685 (1994)
[4] H. Zhu, J. Hobdell, and A. Windle, Acta Mater. **48**, 4893 (2000)
[5] A. Roberts and E. Garboczi, Acta Mater. **49**, 189 (2001)
[6] Y. Gan, C. Chen, and Y. Shen, Int. J. Solids Struct. **42**, 6628 (2005)
[7] W.-Y. Jang, S. Kyriakides, and A. Kraynik, Int. J. Solids Struct. **47**, 2872 (2010)
[8] S. Chiu, D. Stoyan, W. Kendall, and J. Mecke, *Stochastic Geometry and its Applications*, 3rd ed. (Wiley, 2013)
[9] W.-Y. Jang, A. Kraynik, and S. Kyriakides, Int. J. Solids Struct. **45**, 1845 (2008)
[10] A. Al-Kharusi and M. Blunt, J. Petrol. Sci. Eng. **56**, 219 (2007)
[11] A. Liebscher, C. Proppe, C. Redenbach, and D. Schwarzer, Procedia IUTAM **6**, 87 (2012)
[12] I. Vecchio, C. Redenbach, and K. Schladitz, Comp. Mater. Sci. **83**, 171 (2014)
[13] I. Kadashevich and D. Stoyan, Comp. Mater. Sci **43**, 293 (2008)
[14] I. Kadashevich and D. Stoyan, Comput. Concrete **7**, 39 (2010)
[15] A. Roberts and E. Garboczi, J Mech. Phys. Solids **50**, 33 (2002)
[16] S. Feng, M. Thorpe, and E. Garboczi, Phys. Rev. B **31**, 276 (1985)
[17] E. Garboczi, Phys. Rev. B **37**, 318 (1988)
[18] E. Garboczi, Phys. Rev. B **36**, 2115 (1987)
[19] E. Garboczi and M. Thorpe, Phys. Rev. B **32**, 4513 (1985)
[20] M. F. Thorpe and Y. Cai, J. Non-Cryst. Solids **114**, 19 (1989)
[21] M. Thorpe and E. Garboczi, Phys. Rev. B **42**, 8405 (1990)
[22] M. Ostoja-Starzewski and C. Wang, Acta Mech. **80**, 61 (1989)
[23] J. Hansen, R. Skalak, S. Chien, and A. Hoger, Biophys. J. **70**, 1146 (1996)
[24] E. Karpov, N. Stephen, and Liu W.K., Int. J. Solids Struct. **40**, 5371 (2003)
[25] O.C Zienkiewicz and R.L Taylor *The Finite Element Method*, 5th ed. (Butterworth-Heinemann, 2000)
[26] F. Gulminelli, J. M. Carmona, P. Chomaz, J. Richert, S. Jiménez, and V. Regnard, Phys. Rev. E **68**, 026119 (2003)
[27] J. Carmona, J. Richert, and A. Tarancon, Nuc. Phys. A **643**, 115 (1998)
[28] J. Honerkamp, *Statistical Physics*, 3rd ed., Graduate Texts in Physics (Springer, 2012)
[29] K. Mardia and P. Jupp, *Directional Statistics*, Wiley Series in Probability and Statistics (Wiley, 1999)
[30] R. Sok, M. Knackstedt, A. Sheppard, W. Pinczewski, W. Lindquist, A. Venkataangan, and L. Paterson, Transport Porous Med. **46**, 345 (2000)